Expression of DFak56, a *Drosophila* homolog of vertebrate focal adhesion kinase, supports a role in cell migration *in vivo*

George L. Fox*†, Ilaria Rebay†‡, and Richard O. Hynes*†§¶

§Howard Hughes Medical Institute, *Center for Cancer Research, and †Department of Biology, Massachusetts Institute of Technology, Cambridge, MA 02139; and ‡Whitehead Institute for Biomedical Research, Cambridge, MA 02142

Contributed by Richard O. Hynes, October 25, 1999

Focal adhesion kinase (FAK) is a highly conserved, cytoplasmic tyrosine kinase that has been implicated in promoting cell migration and transmission of antiapoptotic signals in vertebrate cells. In cultured cells, integrin engagement with the extracellular matrix promotes the recruitment of FAK to focal contacts and increases in its phosphotyrosine content and kinase activity, suggesting FAK is an intracellular mediator of integrin signaling. We have identified a Drosophila FAK homolog, DFak56, that is 33% identical to vertebrate FAK, with the highest degree of homology in domains critical for FAK function, including the kinase and focal adhesion targeting domains, and several protein–protein interaction motifs. Furthermore, when expressed in NIH 3T3 cells, DFak56 both localizes to focal contacts and displays the characteristic elevation of phosphotyrosine content in response to plating the cells on fibronectin. During embryogenesis, DFak56 is broadly expressed, and it becomes elevated in the gut and central nervous system at later stages. Consistent with a role in cell migration, we also observe that DFak56 is abundant in the border cells of developing egg chambers before the onset of, and during, their migration.

Integrins are a family of cell surface molecules that link the extracellular matrix with the actin cytoskeleton. As such, they are in a position to transmit information into and out of the cell, and it is now well established that integrin-mediated signaling influences many intracellular events, including rearrangement of the actin cytoskeleton, cell migration, cell survival, and gene expression (1, 2). Focal adhesion kinase (FAK) was one of the first molecules identified as playing a role in integrin signaling, and hence it has figured prominently in models of such events. Much of the early work on FAK focused on identifying the molecules with which it interacts, including focal contact and adaptor proteins like talin (3), paxillin (4), and $p130^{cas}$(CAS) (5), and kinases like src (6) and PI3K (7). More recently, it has been observed that increasing the expression of FAK in cells can stimulate both migration (8) and cell survival (9), and further research into these phenomena has emphasized the importance of FAK's interactions with src, PI3K, and CAS (10–13). Ablation of FAK in mouse embryos produces early embryonic lethality, and FAK-null cells show reduced motility (14).

Drosophila offers a genetically tractable system in which to analyze the *in vivo* functions of genes and proteins. Several integrins have been described in *Drosophila*, and the effects of mutations in integrin genes have been analyzed (15, 16). To extend such analysis to downstream signaling molecules, we have identified and cloned a FAK homolog from *Drosophila* and report here on some of its characteristics, including evidence supporting a role in migration *in vivo*.

Materials and Methods

Cloning of cDNAs. PCR was performed on 2λ of template synthesized from 12 μg of Drosophila 0- to 24-hr total embryonic RNA by using the First Strand Synthesis Kit (Promega). In the first round, primers FAKN:5′-ACTGGAATTCGA(C/T)GA(G/A)GA(G/A)GA(T/C)ACITA(T/C)ACIATG-3′ and FAKK1:5′-GG(A/G)TC(A/G)TAIGCCCA(A/G)CA(T/C)TT-3′ were used. The first round product was diluted 1:100 and was mixed with primers FAKN and FAKK2:5′-ACTGGAATTC(G/A)AACATCCAIAC(G/A)TC-3′. These three primers derive from highly conserved sequences located in the kinase domains and N termini of vertebrate FAKs. Primers were used at 3.3 ng/μl in reactions of 40 cycles of 94°C 1′, 50°C 2′, and 72°C 3′. The final PCR product was cloned into pBluescript II SK(+) (Stratagene) and was sequenced (Sequenase Kit, United States Biochemical). A 750-bp *Eco*RI/*Hin*dIII fragment of the PCR clone (bp 930-1680 of the full-length cDNA) was used to probe a λgt11 9- to 13-hr embryonic cDNA library, provided by K. Zinn (California Institute of Technology). Plaques (2.3×10^5) were screened under high stringency conditions, and two positive inserts were subcloned and sequenced.

RNA Analysis. *Developmental Northern blots.* Total RNA (30 μg) from timed developmental stages were electrophoresed and blotted. The blot was hybridized with randomly labeled DNA probes made from the 5′ portion (bp 1–930) or the 3′ untranslated region (UTR) (bp 3,701–4,157), then washed and exposed to film (16). Sense and anti-sense RNA probes were synthesized by using the Dig RNA labeling Kit (Boehringer Mannheim) and were used for *in situ* hybridization (16).

Antibody Production and Use. A *Bsm*I fragment (bp 2,584–3,804) was subcloned into pGEX5x-1 and was transformed into DH5α cells. After induction, cells were sonicated and fusion protein was purified on glutathione agarose (Sigma). Antiserum was generated in guinea pigs by Covance (Richmond, CA) and was used at 1:3,000 in all experiments, except where indicated.

Embryos were collected in 4-hr batches and were fixed (17). Biotinylated goat anti-guinea pig IgG (Jackson ImmunoResearch) was used at 1:200, and signal was visualized with the Vectastain ABC Kit (Vector Laboratories). Egg chambers were fixed and stained as described (18). Texas Red-conjugated goat anti-guinea pig IgG (Jackson ImmunoResearch) was used at 1:200.

Western blots were blocked for 1 hr with 5% blotto (5% milk in PBS + 0.1% Tween-20) and were incubated with guinea pig antiserum overnight. After washes in PBS + 0.1% Tween-20, blots were incubated for 1 hr with horseradish peroxidase-conjugated goat anti-guinea pig IgG (Jackson ImmunoResearch) at 1:5000. Blots were developed with the Renaissance chemiluminescence kit (Dupont/NEN).

Abbreviations: FAK, focal adhesion kinase; UTR, untranslated region; FAT, focal adhesion targeting.

Data deposition: The sequence reported in this paper has been deposited in the GenBank database (accession no. AF201701).

¶To whom reprint requests should be addressed. E-mail: rohynes@mit.edu.

The publication costs of this article were defrayed in part by page charge payment. This article must therefore be hereby marked "*advertisement*" in accordance with 18 U.S.C. §1734 solely to indicate this fact.

Cell Lines. S2 cells were transiently transfected with pCaSpeR-hs or pCaSpeR-hs(DFak56). The following day they were heat-shocked at 37°C for 1 hr. After a 2-hr recovery at 25°C, cells were lysed in gel loading buffer. NIH 3T3 cells were transfected with pMIG or pMIG(DFak56) as described (19). The pMIG vector encodes a viral promoter, multiple cloning site, an internal ribosomal entry site, and green fluorescent protein for sorting by fluorescence-activated cell sorter analysis. After two rounds of selection, >90% of cells are green fluorescent protein-positive.

Fibronectin Assays. For phosphotyrosine analysis, tissue culture dishes were coated with 10 μg/ml human plasma fibronectin or 0.5 mg/ml polylysine overnight at 4°C. Cells (5×10^5) were allowed to adhere for 2 hr at 37°C and then were lysed with RIPA buffer (0.15 M NaCl/0.01 M Tris·HCl, pH 7.3/1 mM EGTA/1% Triton X-100/1% sodium deoxycholate/0.1% SDS). Antibody 44-642 (Biosource International, Camarillo, CA) was used at 1:500. For immunofluorescence, cells were allowed to adhere to fibronectin-coated glass coverslips overnight at 37°C and then

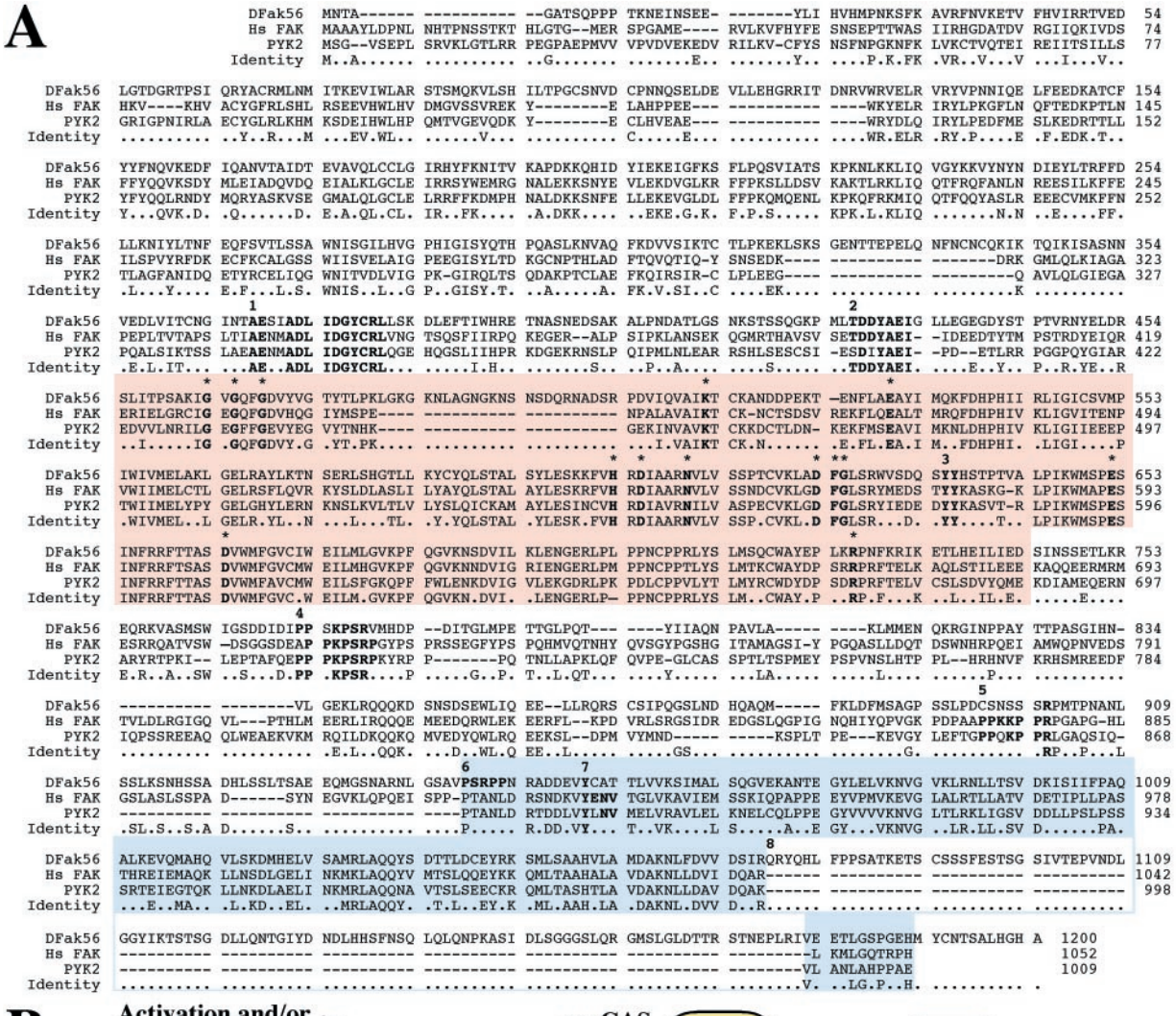

Fig. 1. (*A*) Alignment of the predicted protein sequence of DFak56 with (human) Hs FAK and PYK2. Positions at which DFak56 is identical to either Hs FAK or PYK2 are indicated on the Identity line. The kinase and focal adhesion targeting (FAT) domains are highlighted in red and blue, respectively. Within the kinase domain, 14 residues invariant among all tyrosine kinases have been indicated by bold characters and asterisks. Additional sequences of interest, also in bold, are distinguished by numbers: 1; the most prominent stretch of identity outside the kinase domain; 2, the autophosphorylation site; 3, a dityrosine motif, located in the activation loop of the kinase domain; 4, a proline-rich sequence required for interaction between FAK and CAS; 5, a second proline-rich sequence that has been implicated in interactions with both CAS and Graf; 6, a proline-rich sequence unique to DFak56; 7, a site of src phosphorylation that mediates an interaction with Grb2; and 8, the 104-aa insertion at the end of the FAT domain of DFak56. (*B*) Summary of potential DFak56 interactions predicted by homology. It seems highly likely that DFak56 will interact with signaling molecules such as PI3K, src, and p130^{CAS}, and the focal contact proteins talin and paxillin. The interaction with Grb2, on the other hand, does not seem to be conserved, and an interaction with Graf (assuming that there is a *Drosophila* homolog) seems unlikely.

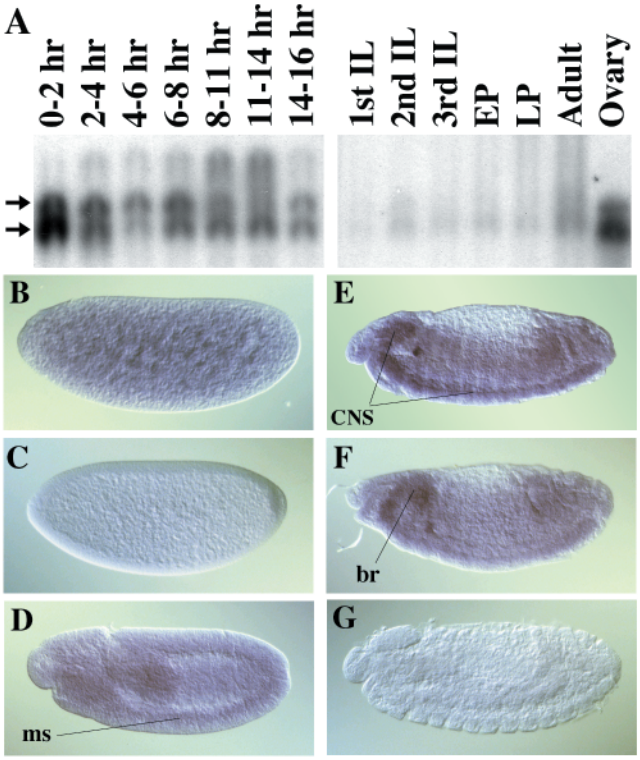

Fig. 2. Expression pattern of DFak56. (*A*) Developmental Northern blot hybridized with a 5′ probe from DFak56 cDNA. Three bands are detected: 4.7, 5.3, and 6.5 kb. The times refer to hours of embryonic development. IL, instar larva; EP and LP, early and late pupa, respectively. The reduction in expression in larval and pupal stages is exaggerated because of loading differences [as determined by a probe to RP49 (not shown)]. (*B–F*). Staged embryos stained with a DFak56 anti-sense RNA probe. Representative examples of stage 3 (*B*), 5 (*C*), 11 (*D*), 13 (*E*), and 14 (*F*) embryos are shown; br, brain; ms, mesoderm. (*G*) A stage 13 embryo stained with a DFak56 sense RNA probe.

were fixed in paraformaldehyde. Primary anti-serum was used at 1:1,000, Texas Red goat anti-guinea pig IgG (Jackson ImmunoResearch) at 1:200, and vinculin anti-serum at 1:100.

Results

Isolation and Analysis of DFak56 cDNAs. By using degenerate PCR, a 1,300-bp partial cDNA was amplified from reverse-transcribed 0- to 24-hr *Drosophila* embryonic RNA. Sequencing indicated the presence of a kinase domain most similar to the FAK subfamily of tyrosine kinases. By using the 5′ end of this clone as a probe, a full-length cDNA was isolated from a λgt11 9- to 13-hr library. The corresponding mRNA consists of a 91-bp 5′UTR, a 3,600-bp ORF, and a 455-bp 3′UTR. The 1,200-aa predicted protein is most similar to vertebrate FAKs. Because the gene localizes to polytene band 56D by *in situ* hybridization (data not shown), it is designated as DFak56. Genomic sequence submitted by the Berkeley Drosophila Genome Project confirms both the sequence and the polytene localization.

The vertebrate FAK family consists of two subgroups, canonical FAK proteins and the somewhat divergent PYK2 proteins (20–22). Alignment of DFak56 with a representative member of each subgroup suggests it is a member of the FAK subfamily. Over its entire length, DFak56 is 33% identical to members of the FAK subgroup and 29% identical to members of the PYK2 subgroup; the conservation of known functional domains is significantly stronger. For example, the kinase domain of DFak56 is 57.4% identical to that of human (Hs) FAK and 48.8% identical to that of PYK2, and the focal adhesion targeting (FAT) domain of DFak56 is 43.3% identical to the FAT domain of Hs FAK and 39.0% identical to the FAT domain of PYK2. In the kinase domain, the 14 residues invariant in the tyrosine kinase superfamily are all conserved (Fig. 1, asterisks), and the 24-aa insertion occurs in a loop known to vary among tyrosine kinases (23, 24). An interesting difference between DFak56 and other FAK family members is that DFak56 contains a 104-aa insertion close to the C-terminal end of its FAT domain (Fig. 1, 8). This insert is not homologous with known sequences.

In addition to the kinase and FAT domains, a number of short peptide sequences that mediate known protein–protein interactions have been conserved among DFak56 and vertebrate FAKs. The autophosphorylation site (Fig. 1, 2), which comprises a binding site for the SH2 domain of either src or PI3K, is well conserved. Other conserved sequences include the dityrosine motif located in the activation loop of the kinase domain (Fig. 1, 3) and the proline-rich sequence immediately C-terminal to the kinase domain (Fig. 1, 4). Phosphorylation of the dityrosine motif has been correlated with increased kinase activity (25), and its substitution with a diphenylalanine motif results in impaired activation of the FAK/src complex and reduced cell spreading and migration (10). The proline-rich sequence is the primary binding site for the SH3 domain of CAS, and the resulting interaction is believed to play an important role in stimulating cell migration (12, 26) and suppressing apoptosis (27). Finally, the N terminus, shown *in vitro* to bind the cytoplasmic tail of β1 integrins and thought to play a role in FAK activation (28, 29), contains a striking stretch of identity not previously noted (Fig. 1, 1). When placed on an α-helical wheel, this sequence has an amphipathic structure (not shown).

A second C-terminal proline-rich sequence present in vertebrate FAKs, and implicated as a secondary binding site for CAS (26) and a primary binding site for Graf, a rho-GAP (30), is not present in DFak56 (Fig. 1, 5). There is, however, a proline-rich sequence that is unique to DFak56 at the beginning of its FAT domain (Fig. 1, 6). This sequence, PSRPP, is quite similar to the first proline-rich sequence, PPSKP, suggesting that it may act as the secondary binding site for CAS in DFak56. Finally, DFak56 appears to lack the SH2 domain binding site for Grb2 (Fig. 1, 7). A summary of this information is shown in Fig. 1*B*.

Temporal Expression Pattern of DFak56. To determine when DFak56 is expressed during development, we hybridized a developmental Northern blot with a probe from the 5′ end of the DFak56 cDNA and detected three bands at 4.7, 5.3, and 6.5 kb (Fig. 2*A*). The 4.7- and 5.3-kb transcripts (arrows) are expressed during all developmental stages examined, but most notably during embryogenesis. During larval and pupal stages, expression is reduced. Note also the high level of expression in ovaries (Fig. 2*A*). The abundance of these messages in both 0- to 2-hr embryos and ovaries suggests a maternal contribution. The 6.5-kb message is present at comparatively low levels during development but is up-regulated at 8- to 14-hr of embryogenesis. Identical results were obtained with a DFak56 3′UTR probe (not shown).

Spatial Expression Pattern of DFak56 in Embryos. *In situ* hybridization to *Drosophila* embryos was performed by using a biotinylated anti-sense RNA probe (Fig. 2 *B–F*). At early stages of development (Fig. 2 *B–D*), DFak56 is expressed throughout the embryo. After cellularization, there is an abrupt, yet transient, drop in the level of mRNA in the blastoderm (Fig. 2*C*). Expression levels increase during gastrulation (Fig. 2*D*), with highest levels in the mesoderm. At stage 13, DFak56 mRNA decreases in some cells, giving rise to a pattern of segmental stripes, and enriched expression in the gut and central nervous system becomes apparent (Fig. 2*E*). By stage 14, the expression pattern is once again uniform, with the exception of elevated

expression in the brain (Fig. 2*F*). Embryos stained with a sense RNA control probe (Fig. 2*G*) showed little or no staining.

Localization of DFak56 Protein in Embryos. We raised guinea pig antibodies against the C-terminal domain of DFak56 (see below) and stained embryos. Consistent with the mRNA expression pattern, DFak56 protein is uniformly distributed during early embryogenesis (Fig. 3 *A–D*), although there is no drop in protein levels after cellularization of the blastoderm (Fig. 3*B*). Expression increases in the central nervous system and gut during stage 13 (Fig. 3*E*), and these heightened levels persist through stage 15 (Fig. 3*F*) and beyond. A ventral view of a stage 16 embryo reveals more clearly the elevated levels of DFak56 protein in the gut and central nervous system, as well as variation in protein concentration along the length of the body wall (Fig. 3*G*). This variation first appears at stage 15 (not shown). Examination of the body wall from stage 16 embryos at higher magnification shows that our antiserum does not detect accumulation of DFak56 protein in muscle attachment sites (Fig. 3*H*, arrows), although there is a striking decrease in signal in ectodermal cells located at the segmental boundaries (*I*, arrows).

DFak56 Is Abundant in the Migrating Border Cells of Developing Egg Chambers. Given the presence of DFak56 mRNA in ovaries (Fig. 2*A*), we stained developing egg chambers with DFak56 antiserum. DFak56 is abundant in the germ cells at early stages of oogenesis, but decreases significantly by stage 6 (Fig. 4*A*). A similar, but less dramatic, decrease occurs in the somatic follicle cells, but they continue to express DFak56 at later stages (Fig. 4 *B–D*). Strikingly, the level of DFak56 does not drop in follicle cells at the anterior end of stage 6 egg chambers (Fig. 4*A*, arrows, and Fig. 4*B*). An enlarged view of the anterior tip of the stage 6 egg chamber (Fig. 4*A Inset*) shows more clearly the difference in DFak56 levels between follicle cells at the anterior tip and those more posterior.

This elevated level of DFak56 protein persists through early stage 9, when a group of follicle cells, known as the border cells, begin to migrate between the nurse cells toward the oocyte (31). The border cells originate from the anterior tip of the egg chamber and thus contain high levels of DFak56 protein (Fig. 4*B*, arrow). DFak56 is prominent in the border cells throughout their migration (Fig. 4 *C* and *D*, arrows). Notably, DFak56 does not localize to ring canals in which elevated levels of phosphotyrosine and F-actin have been reported (32). It does, however, seem to accumulate in the basal region of the posterior follicle cells (Fig. 4 *B* and *C*, arrowheads).

Characterization of DFak56 Antibodies. Antisera, raised against the C terminus of DFak56, were obtained from two guinea pigs. They produced identical results in all assays (not shown) and recognize a 140-kDa band (the predicted size of DFak56 protein) on Western blots whereas preimmune sera do not (Fig. 5*A*). The 140-kDa band increases in intensity in extracts of S2 cells transfected with pCaSpeR-hs(DFak56) and heat-shocked, demonstrating the specificity of the antisera.

DFak56 Is Functionally Conserved. To test how the functions of DFak56 compare with those of vertebrate FAK, we used a retroviral expression construct containing DFak56 to infect NIH 3T3 cells. Upon infection, the cells express DFak56 at high levels (Fig. 5*B*). When these cells are plated on fibronectin, DFak56 becomes phosphorylated (Fig. 5*B*). In contrast, when the cells are plated on polylysine or kept in suspension, DFak56 displays much less phosphorylation (Fig. 5*B*). This phosphorylation profile mirrors that of the endogenous mouse FAK, distinguishable by its smaller size. Thus, DFak56 appears to be activated in response to an integrin-mediated signal. DFak56 localizes to focal contacts when these cells are plated on fibronectin (Fig. 5*C*).

Discussion

We have identified a new member of the focal adhesion kinase family of tyrosine kinases from Drosophila, DFak56. As we were about to submit this paper, a paper by Fujimoto *et al.* (33) appeared also reporting the cloning of DFak56. Their sequence agrees with ours, that of Palmer *et al.* (34), and the genomic sequence reported by the Berkeley Drosophila Genome Project, except for minor discrepancies.

Among conserved sequence motifs (see Fig. 1 and *Results*), we note particularly the previously unrecognized motif in the N-

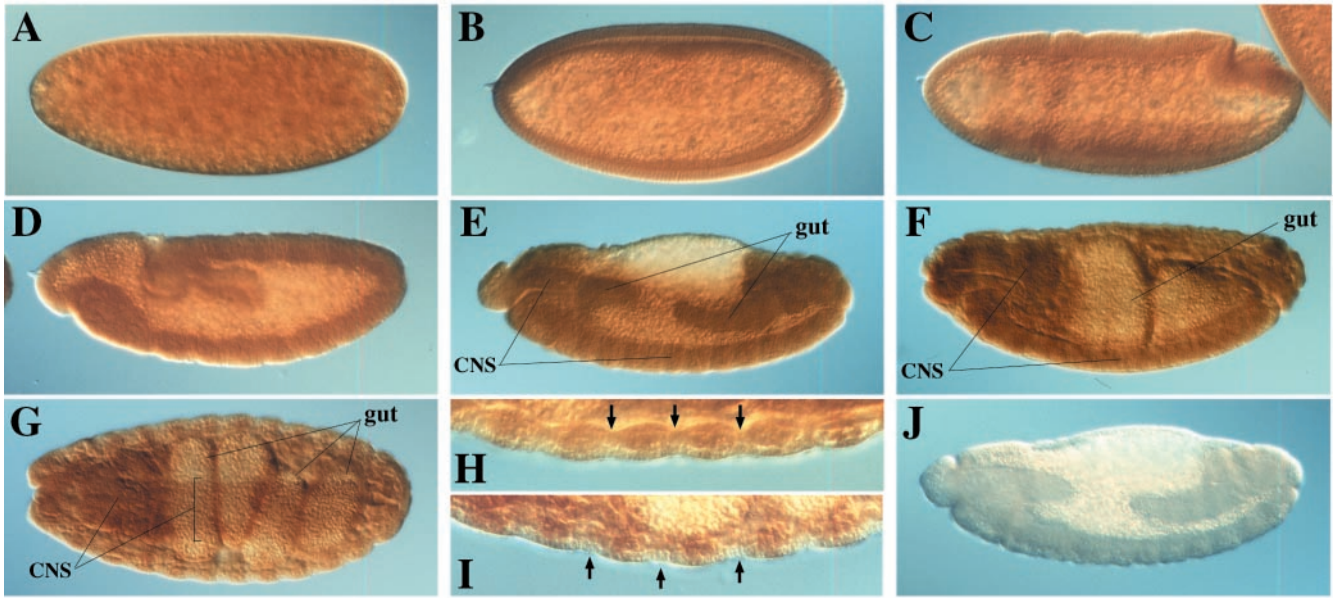

Fig. 3. Localization of DFak56 protein during embryogenesis. Polyclonal anti-serum 1562C, raised against the C terminus of DFak56, was used to stain fixed embryos: stage 3 (*A*), 5 (*B*), 6 (*C*), 11 (*D*), 13 (*E*), 15 (*F*), and 16 (*G*, seen from the ventral side). Magnified ventral views of stage 16 embryos are shown in *H* and *I*; arrows indicate muscle attachment sites (*H*) and ectodermal cells located at segmental junctions (*I*). Preimmune serum gave little or no signal (*J*).

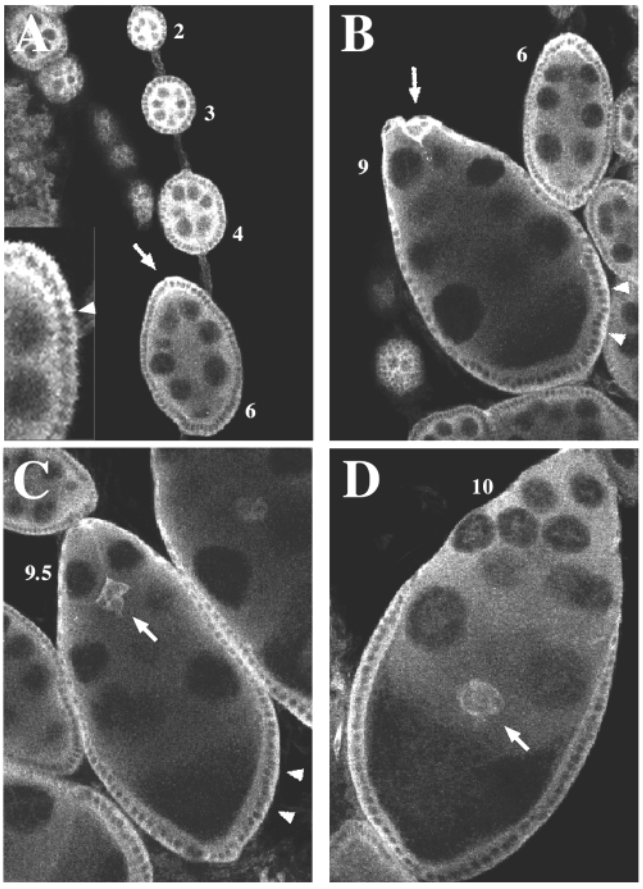

Fig. 4. Confocal images of egg chambers stained for DFak56 protein. (*A*) Stage 2 to stage 6 egg chambers (see numbers). The arrow indicates the anterior tip of the stage six egg chamber, and the inset shows an enlarged view of the right side of the anterior tip, slightly rotated. The arrowhead marks the boundary between high and low expression. (*B*) At early stage 9, border cells (arrow) begin to migrate between the nurse cells toward the oocyte at the posterior end of the egg chamber. Their migration continues through mid-stage 9 (*C*), and they reach the oocyte during stage 10 (*D*). Arrowheads in *B* and *C* indicate follicle cells at the posterior ends of the egg chambers. Control egg chambers stained with preimmune serum show a much lower, uniform signal (not shown).

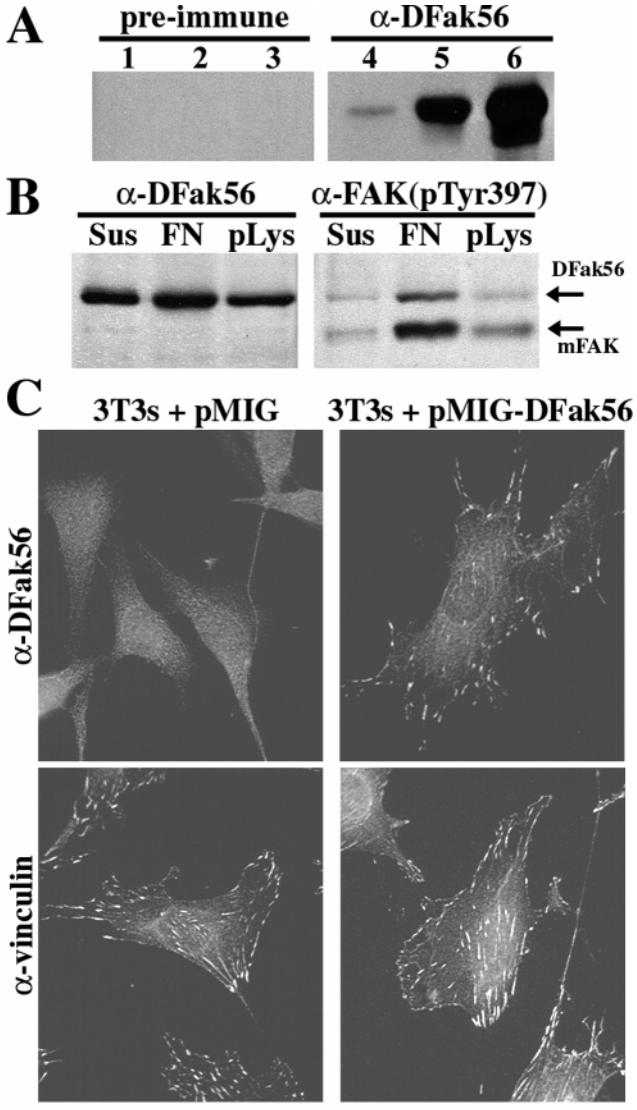

Fig. 5. DFak56 functions like endogenous FAK in NIH 3T3 cells. (*A*) Western blots of 100 μg of embryo extract (lanes 1 and 4), and 33 μg of extract from S2 cells transfected with pCaSpeR-hs (lanes 2 and 5) or S2 cells transfected with pCaSpeR-hs(DFak56) (lanes 3 and 6). Identical blots were probed with antiserum 1563C (α-DFak56) or preimmune serum. 1563C recognizes a 140-kDa band (the predicted size of DFak56) in protein extracts from both embryos and S2 cells whereas the preimmune serum does not. The increase in signal in this band when S2 cells are transfected with pCaSpeR-hs(DFak56) and heat-shocked (compare lanes 5 and 6) demonstrates specificity for DFak56. Similar results were obtained with antiserum 1562C (not shown). (*B*) Western blots of protein extracts from NIH 3T3 cells infected with pMIG-DFak56, a retroviral expression vector. Equal numbers of infected cells were maintained in suspension (Sus), were plated on fibronectin (FN), or were plated on poly-lysine (pLys) for 2 hr and were lysed. Identical blots were probed with either 1563C (α-DFak56) or a polyclonal antiserum specific to the phosphorylated form of the FAK autophosphorylation site [α-FAK(pTyr397)]. (*C*) Subcellular localization of DFak56 in NIH 3T3 cells infected with either the empty retroviral vector, pMIG (*Left*) or pMIG-DFak56 (*Right*). Cells were allowed to adhere to fibronectin overnight and were fixed and stained with 1563C (α-DFak56) or an anti-vinculin antiserum.

terminal segment (Fig. 1, 1). The strong conservation of this motif indicates an important function. Conservation in Pyk2 perhaps argues against a role in association with integrins. Other functional motifs characterized in vertebrate FAKs are conserved in DFak56. At the functional level, DFak56 transfected into mammalian cells localizes to focal contacts (Fig. 5*C*) and becomes activated when the cells are plated on fibronectin (Fig. 5*B*), behaviors characteristic of the canonical FAKs. It is interesting to note that, for each domain examined, DFak56 shares greater homology with Hs FAK than with PYK2.

Placement of DFak56 in the FAK subgroup is further substantiated by three additional findings. First, a phylogenetic tree produced by aligning only the kinase domains groups DFak56 with the canonical FAKs and identifies the PYK2 subgroup as most divergent (not shown). Second, if we include in our comparative analysis of the FAT domain 50 amino acids on the N-terminal side, we observe that DFak56 is 38.2% identical to human FAK and 29.3% identical to PYK2. This variation is quite significant, given that FAK and PYK2 differ in their subcellular localization and response to integrin signaling, and that these differences largely depend on the properties of their FAT domains (35). Third, at the positions just before the autophosphorylation site tyrosine, the sequence of DFak56 matches that of Hs FAK but not PYK2 (Fig. 1, 2). These residues have been shown to be critical for the association with PI3K (11), and differences in them may explain why PYK2 is unable to compensate fully for loss of FAK activity in FAK-null cells (36). We conclude that DFak56 is the *Drosophila* ortholog of vertebrate FAK

DFak56 mRNA is widely expressed in embryos, and at later stages there is elevated expression in the gut and central nervous system. This developmental expression pattern is similar to that described for *Xenopus* FAK (21). An exception to the general expression pattern of DFak56 mRNA is the reduction that occurs in thin stripes of cells on the lateral surfaces of embryos during stage 13 (Fig. 2*E*). We observe a similar decrease in DFak56 protein in epidermal cells located at segmental junctions later, during stages 15 and 16 (Fig. 3*I*). However, Fujimoto *et al.* (33) reported a high level of expression in the tendon cells of the lateral epidermis and a correspondingly high concentration of DFak56 protein in muscle attachment sites. We have not observed this; the bases for the discrepancies are unclear. Whereas Fujimoto *et al.* used a full-length *in situ* probe, ours included only the 3′ 3,220 bp of our cDNA. With respect to protein localization, the main difference is that their antibody was raised against the N terminus whereas ours is specific to the C terminus. How this could create such a big difference in results is unclear. It is possible that our antibody is somehow occluded from muscle attachment sites or that their finding represents a novel function for the N-terminal domain of DFak56.

Our Northern blot results also differ somewhat from those of Fujimoto *et al.* Specifically, they reported a 1.5-kb transcript detected by a full length probe, but not by a 5′ probe. They suggest that this transcript comes from the 3′ end of DFak56 and that it encodes a C-terminal fragment. However, using a 3′UTR probe, we did not detect such a transcript. Furthermore, our antibodies against the C-terminal segment do not detect anything other than the full-length protein on Western blots, arguing against expression of a C-terminal fragment of DFak56, in contrast with the situation in vertebrates.

We have detected abundant DFak56 protein in the border cells of developing egg chambers, both before and during their migration. This correlation is consistent with the proposed role for FAK in promoting cell migration, but it forces the question: Why is DFak56 not also up-regulated in other migrating cells, such as pole cells? There are probably other signaling molecules that promote migration, as suggested by the ability of FAK-null cells to migrate (14), and different environments may require different balances of such pro-migratory signals. We did not observe a concentration of DFak56 at ring canals in the ovary (Fig. 4) despite the concentration there of F-actin and phosphotyrosine, reminiscent of the situation at focal contacts in vertebrates (32).

Altogether, our data suggest that DFak56 is structurally more closely related to canonical FAKs and should provide a useful genetic model for investigating FAK function. It will be important to generate a DFak56 mutant to enable analysis of FAK's role in development and integrin signaling and its contribution to other signaling pathways. We have generated P-element insertions close to the DFak56 locus, but the region is very crowded, with several closely linked genes, and it is not yet possible to assign defects to specific genes (ref. 34; G.L.F., unpublished data).

Special thanks to Rachna Ram for support and encouragement. Thanks also to the Berkeley Drosophila Genome Project for genomic sequence. This work was supported by a grant from National Cancer Institute (RO1CA1707) and by the Howard Hughes Medical Institute (R.O.H.). G.L.F. was supported by National Institutes of Health Grant GM07287. I.R. is a recipient of a Burroughs Wellcome Fund Career Award in the Biomedical Sciences and is a Rita Allen Foundation Scholar. R.O.H. is an Investigator of the Howard Hughes Medical Institute.

1. Cary, L. A., Han, D. C. & Guan, J. L. (1999) *Histol. Histopathol.* **14,** 1001–1009.
2. Clark, E. A. & Brugge, J. S. (1995) *Science* **268,** 233–239.
3. Chen, H. C. & Guan, J. L. (1994) *Proc. Natl. Acad. Sci. USA* **91,** 10148–10152.
4. Hildebrand, J. D., Schaller, M. D. & Parsons, J. T. (1995) *Mol. Biol. Cell.* **6,** 637–647.
5. Polte, T. R. & Hanks, S. K. (1995) *Proc. Natl. Acad. Sci. USA* **92,** 10678–10682.
6. Xing, Z., Chen, H. C., Nowlen, J. K., Taylor, S. J., Shalloway, D. & Guan, J. L. (1994) *Mol. Biol. Cell.* **5,** 413–421.
7. Chen, H. C., Appeddu, P. A., Parsons, J. T., Hildebrand, J. D., Schaller, M. D. & Guan, J. L. (1995) *J. Biol. Chem.* **270,** 16995–16999.
8. Cary, L. A., Chang, J. F. & Guan, J. L. (1996) *J. Cell Sci.* **109,** 1787–1794.
9. Frisch, S. M., Vuori, K., Ruoslahti, E. & Chan-Hui, P. Y. (1996) *J. Cell Biol.* **134,** 793–799.
10. Owen, J. D., Ruest, P. J., Fry, D. W. & Hanks, S. K. (1999) *Mol. Cell. Biol.* **19,** 4806–4818.
11. Reiske, H. R., Kao, S. C., Cary, L. A., Guan, J. L., Lai, J. F. & Chen, H. C. (1999) *J. Biol. Chem.* **274,** 12361–12366.
12. Sieg, D. J., Hauck, C. R. & Schlaepfer, D. D. (1999) *J. Cell Sci.* **112,** 2677–2691.
13. Sonoda, Y., Watanabe, S., Matsumoto, Y., Aizu-Yokota, E. & Kasahara, T. (1999) *J. Biol. Chem.* **274,** 10566–10570.
14. Ilic, D., Furuta, Y., Kanazawa, S., Takeda, N., Sobue, K., Nakatsuji, N., Nomura, S., Fujimoto, J., Okada, M., Yamamoto, T. & Aizawa, S. (1995) *Nature (London)* **377,** 539–544.
15. Brower, D. L., Brabant, M. C. & Bunch, T. A. (1995) *Immunol. Cell Biol.* **73,** 558–564.
16. Stark, K. A., Yee, G. H., Roote, C. E., Williams, E. L., Zusman, S. & Hynes, R. O. (1997) *Development (Cambridge, U.K.)* **124,** 4583–4594.
17. Kidd, S., Baylies, M. K., Gasic, G. P. & Young, M. W. (1989) *Genes Dev.* **3,** 1113–1129.
18. Cant, K., Knowles, B. A., Mooseker, M. S. & Cooley, L. (1994) *J. Cell Biol.* **125,** 369–380.
19. Liu, X., Sun, Y., Constantinescu, S. N., Karam, E., Weinberg, R. A. & Lodish, H. F. (1997) *Proc. Natl. Acad. Sci. USA* **94,** 10669–106674.
20. Whitney, G. S., Chan, P. Y., Blake, J., Cosand, W. L., Neubauer, M. G., Aruffo, A. & Kanner, S. B. (1993) *DNA Cell Biol.* **12,** 823–830.
21. Hens, M. D. & DeSimone, D. W. (1995) *Dev. Biol.* **170,** 274–288.
22. Yu, H., Li, X., Marchetto, G. S., Dy, R., Hunter, D., Calvo, B., Dawson, T. L., Wilm, M., Anderegg, R. J., Graves, L. M. & Earp, H. S. (1996) *J. Biol. Chem.* **271,** 29993–29998.
23. van der Geer, P., Hunter, T. & Lindberg, R. A. (1994) *Annu. Rev. Cell Biol.* **10,** 251–337.
24. al-Obeidi, F. A., Wu, J. J. & Lam, K. S. (1998) *Biopolymers* **47,** 197–223.
25. Calalb, M. B., Polte, T. R. & Hanks, S. K. (1995) *Mol. Cell. Biol.* **15,** 954–963.
26. Cary, L. A., Han, D. C., Polte, T. R., Hanks, S. K. & Guan, J. L. (1998) *J. Cell Biol.* **140,** 211–221.
27. Chan, P. C., Lai, J. F., Cheng, C. H., Tang, M. J., Chiu, C. C. & Chen, H. C. (1999) *J. Biol. Chem.* **274,** 26901–26906.
28. Schaller, M. D., Otey, C. A., Hildebrand, J. D. & Parsons, J. T. (1995) *J. Cell Biol.* **130,** 1181–1187.
29. Chan, P. Y., Kanner, S. B., Whitney, G. & Aruffo, A. (1994) *J. Biol. Chem.* **269,** 20567–20574.
30. Hildebrand, J. D., Taylor, J. M. & Parsons, J. T. (1996) *Mol. Cell. Biol.* **16,** 3169-3178.
31. Montell, D. J. (1999) *Development (Cambridge, U.K.)* **126,** 3035–3046.
32. Robinson, D. N., Cant, K. & Cooley, L. (1994) *Development (Cambridge, U.K.)* **120,** 2015–2025.
33. Fujimoto, J., Sawamoto, K., Okabe, M., Takagi, Y., Tezuka, T., Yoshikawa, S., Ryo, H., Okano, H. & Yamamoto, T. (1999) *J. Biol. Chem.* **274,** 29196–29201.
34. Palmer, R. H., Fessler, L. I., Edeen, P. T., Madigan, S. J., McKeown, M. & Hunter, T. (1999) *J. Biol. Chem.*, in press.
35. Zheng, C., Xing, Z., Bian, Z. C., Guo, C., Akbay, A., Warner, L. & Guan, J. L. (1998) *J. Biol. Chem.* **273,** 2384–2389.
36. Sieg, D. J., Ilic, D., Jones, K. C., Damsky, C. H., Hunter, T. & Schlaepfer, D. D. (1998) *EMBO J.* **17,** 5933–5947.